Analysis of Stress Concentrations in 2x2 Braided Composites

D. Goyal[1], J. D. Whitcomb[1]

Summary

The stress distribution in braided composites is complex even for simple uni-axial loading. The interlacing of the tows creates a complex load path that results in full 3D stress distributions. The location and magnitude of peak stresses depend on the particular stress component and vary with various braid architecture parameters such as braid angle and degree of waviness. Finite element analyses for braids were performed and it was seen that the peak stresses in the tow mainly occur at the undulating region and along the edges of the tow. A considerable volume of the tow (9-45% for the considered range of parameters) had stresses larger than an "equivalent lamina". The percentage volume of the tow that has stresses larger than those in an equivalent lamina decreases with decrease in waviness ratio for most of the cases.

Introduction

Braided composites have a wide variety of applications in aerospace, sports, automobile and medical industries. They are attractive because of the potential for net shape fabrication, associated reduction in part count, and high performance. Figure 1 shows the idealized microstructure of 2x2 braids, which are the focus of this paper. The matrix pockets have been removed to reveal the tows. The fiber preforms can be tailored to create composites of the desired thickness. The dry preform is then impregnated with resin and cured to create a composite.

The fact that tows are interlaced, have undulating and straight regions, and are not orthogonal to each other, causes a complex load path and complex three dimensional stress distributions even for simple uni-axial loading. To properly interpret the predicted stress distributions requires that one has understanding of the cause for the stress concentration. A significant concern is whether some stress concentrations appear only due to the peculiarities of a particular geometric approximation. Also, an intuitive understanding of why stress concentrations occur will allow one to attempt to design away or at least reduce the magnitudes. Due to geometric complexities, relatively little effort has been made to predict the failure behavior of textiles composites. There has been limited progress in predicting the progressive failure of woven composites. Most of the work has been done for the plain weave [1-5]. Various parameters like type of loading, material properties, braid angle, waviness ratio, cross-section shape, and

---

[1]Center for Mechanics of Composites, Aerospace Engineering Department, Texas A&M University, College Station, TX 77843-3141, USA

stacking sequence etc. affect the stress distributions in braids. Due to the space limitations, here we will explore only the effect of braid angle and waviness ratio. Detailed 3D finite element models will be analyzed to determine the effect of these parameters on stress distributions in braids. An equivalent tape laminate model will also be used to normalize the stress results so that the effect of tow orientation can be eliminated.

Configurations

The effect of various parameters on stress distributions in a symmetrically stacked braid was studied. Uni-axial loading was applied along the longitudinal direction (see Figure 1-2). Overall fiber volume fraction in the model was assumed to be 50%. The braid angle (BA) is the angle between the axis of the tow and longitudinal direction of the braid and is shown in Figure 1. The range of braid angle considered in these studies was ±25˚ to ±65˚. The waviness ratio (WR) is a measure of undulation or crimp in the tows. It is defined as the ratio of the height h to the wavelength λ (Figure 2). Very low (1/9), moderate (1/6) and very high (1/3) waviness ratios were considered.

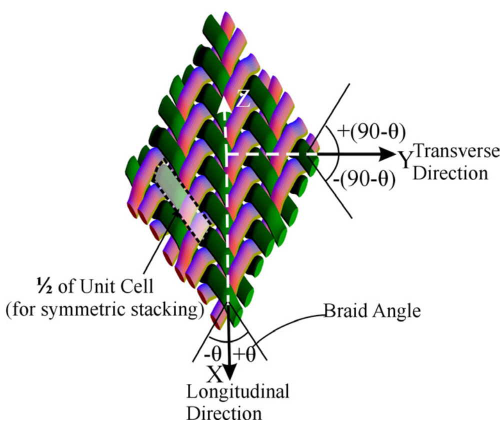

Figure 1. Microstructure of a 2x2 braid

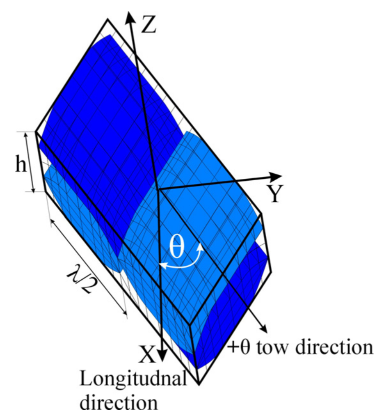

Figure 2. Typical finite element model (matrix transparent to reveal architecture)

The material system used consists of AS4 carbon fibers and EPON epoxy resin. The material properties were taken from ref [6]. The resin is isotropic with E=2.96GPa and υ=0.38. The fiber is transversely isotropic with the following properties: E_{11}=227.53GPa, E_{22}=E_{33}=16.55GPa, G_{12}=G_{13}=24.82GPa, G_{23}=6.89GPa, υ_{12}=υ_{13}=0.2, and υ_{23}=0.25, where the 1 direction is along the fibers. The symbols E, G, υ refer to extensional modulus, shear modulus and Poisson's ratio respectively. The fibers were assumed to be arranged in a hexagonal array in the tow and the properties of the tow were calculated using finite element analysis. The fiber fraction in the tow was assumed to be 0.69. The properties of the tow were determined to be: E_{11}=157.9GPa, E_{22}=E_{33}=9.088GPa, G_{12}=G_{13}=4.839GPa, G_{23}=3.276GPa, υ_{12}=υ_{13}=0.251, υ_{23}=0.4117.

A typical finite element model used for the studies consists of 20-node brick elements and is shown in Figure 2. This model is one-fourth of the unit cell and sufficed for analysis because periodicity of the microstructure and mirroring and rotational symmetries within the unit cell were exploited [7]. The boundary conditions consist of numerous multipoint constraint relations and are given in ref [8]. A typical finite element model used in these studies consists of 1152 elements and 5008 nodes.

A tape laminate model corresponding to each ±θ braid configuration was used to normalize the stresses in the tow. The stacking sequence for the laminate model is $[+\theta_{tow}/-\theta_{tow}/0^o_{resin}]_S$. In this laminate, four layers have properties of the tow and the rest have properties of the matrix to account for matrix pockets in the braid model. The layer thicknesses were consistent with the tow/matrix volume fraction in the braid model. The laminate model was used to eliminate the effect of in-plane orientation of the tows and to quantify the severity of the stresses in the braid as compared to stresses in a corresponding tape laminate. The same amount of load was applied to both the laminate and the braid.

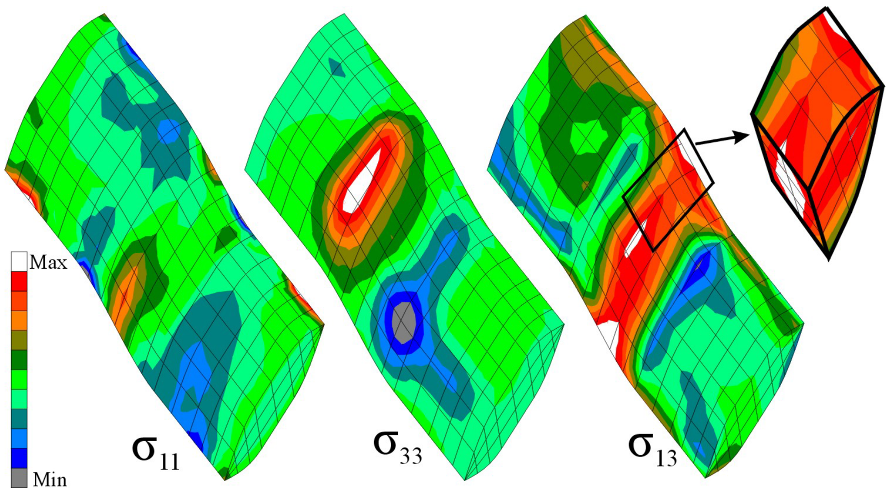

Figure 3. Stress contours in +25˚ braid tow (WR=1/3)

Results and discussions

Figure 3 shows the locations of peak stresses when uni-axial load along the longitudinal direction is applied to a ±25˚ braid with WR of 1/3. Even for simple loading like this, a three dimensional stress state exists in the tow and any stress component could be critical, depending upon the allowables. Figure 3 shows the contours for σ_{11}, σ_{33} and σ_{13} stress components. Complex stress gradients exist for σ_{22}, σ_{12} and σ_{23} also, but the results are not shown here due to space limitations. The σ_{11} stress peaks in the tow are tensile for all the braid angles. In contrast, the peaks for σ_{22} are compressive for ±25˚ and tensile for ±45˚ and ±65˚, which is consistent with laminate theory analysis. For all the braid configurations, there were significant tensile and compressive σ_{33} concentrations. However, for a ±65˚ braid, tensile peaks were much larger than the compressive peaks. The location of tensile peaks for σ_{33} changes from mid of the tow (like that in Figure 3) to the edge of the tow with increase in BA. Peaks for σ_{12} lie on the edge of the tow. The σ_{13} is the only component whose peaks cut through the middle of the tow from top to bottom as shown in Figure 3. For the rest of the stress components the peaks are only on the surface of the tow.

The percentage of the tow having very high value of stresses is typically quite small. Hence, one needs to determine what percentage of the tow exceeds a certain stress level.

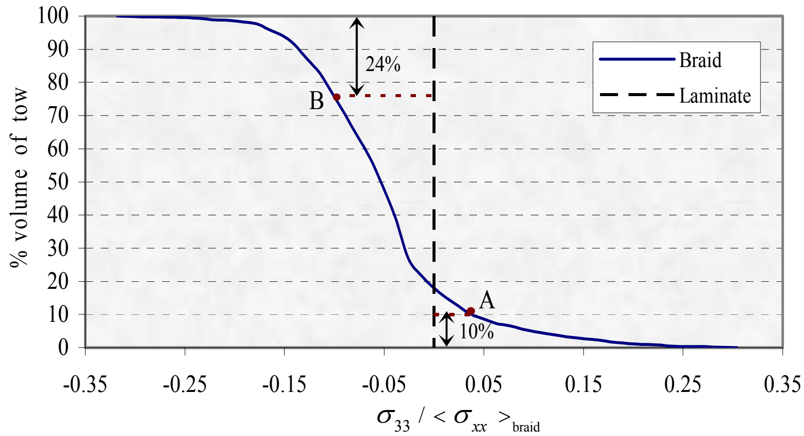

Figure 4. Volume distribution of σ_{33}

A volume distribution plot quantifies the percentage of the volume of the material that is stressed more than a particular value. Figure 4 shows a typical volume distribution plot of σ_{33} in the +θ tow of a ±30˚ braid with waviness ratio =1/3 when uni-axial load is applied. The σ_{33} is normalized by the applied stress. The figure shows that 18% of the volume of the tow has a tensile σ_{33}. Point A, which is in the tensile region, indicates that 10% of the volume has a σ_{33} that is larger than 0.037 times the applied stress. Point B, which is in the compressive region, indicates that 24% of the volume has a compressive stress larger than 0.1 times the magnitude of applied stress. Figure 5 shows the volume distribution of in-plane normal stresses in the +θ tow of ±25˚ and ±45˚ braids. In each plot, the volume distribution curves correspond to waviness ratios 1/3, 1/6 and 1/9 and the vertical straight line corresponds to the constant stress value in the +θ lamina of an equivalent tape laminate. The stresses shown in the figure are normalized with the corresponding absolute +θ lamina values. That is, the plots show

σ_{11}_tow$/|\sigma_{11}$_lamina$|$ and σ_{22}_tow$/|\sigma_{22}$_lamina$|$. Figure 5(a) shows the volume distribution of σ_{11} for several braids. The figure shows that 40% of the tow has larger σ_{11} than an equivalent lamina for a ±25˚ braid for WR =1/3. When the waviness ratio is reduced to 1/9, only 16% of the tow has larger σ_{11} than an equivalent lamina. These percentages change to 18% and 12.5% for a ±45˚ braid for WR = 1/3 and 1/9 respectively (Figure 5(a)). The sensitivity to WR decreased when the braid angle was increased. Figure 5(b) shows the volume distribution of σ_{22}. A ±25˚ braid mainly has compressive σ_{22} stress whereas a ±45˚ braid mainly has tensile σ_{22} stress in the +θ tow. This is consistent with the laminate theory analysis. Figure 5(b) shows that 44.5% of the tow has larger σ_{22} than an equivalent lamina for a ±25˚ braid for WR =1/3.When the waviness ratio is reduced to 1/9, this percentage drops to 36%. These percentages change to 31.5% and 18.5% for a ±45˚ braid for WR =1/3 and 1/9 respectively (Figure 5(b)). The percentage of the tow that has larger in-plane stresses than those in an equivalent lamina is herein referred to as the severity of the stresses in the tow. The severity increases with an increase in WR for ±25˚ and ±45˚ braids for all in-plane stresses. But for a ±65˚ braid, the severity decreased with an increase in WR for σ_{12} and remained almost constant for σ_{11} and σ_{22}. For the considered range of BA (±25˚- ±65˚) and WR (1/9-1/3), 12.5 - 40% of the tow has larger σ_{11} than an equivalent lamina, 18.5 - 44.5% of the tow has larger σ_{22} than an equivalent lamina and 9 - 34% of the tow has larger σ_{22} than an equivalent lamina.

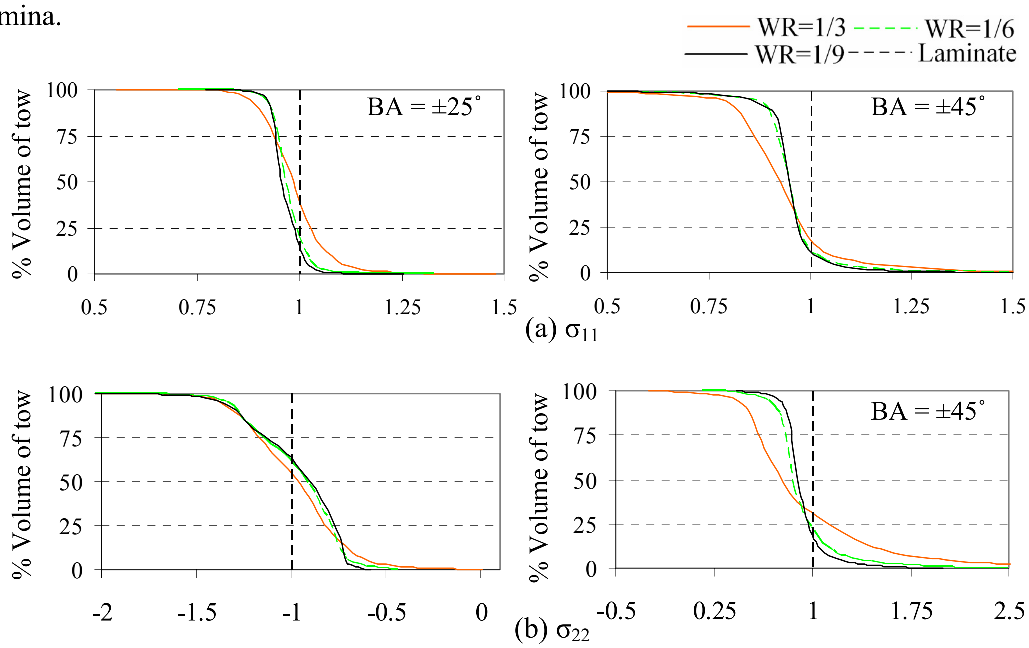

Figure 5: Effect of BA and WR on volume distribution of stresses. Normalized stress ($\sigma_{tow}/|\sigma_{lamina}|$) in the tow versus percentage volume of the tow exceeding a particular value is plotted.

The in-plane stresses in the lamina of a tape laminate are constant, but the value of each stress component varies significantly at different locations in the tow. In general, with an increase in waviness ratio the volume distribution curve tends to broaden in the horizontal direction.

Conclusions

The stress distributions in 2x2 braided composites were analyzed. It was seen that even for simple uni-axial loading, a complex three dimensional stress state exists in the braid. Various parameters like braid angle and waviness ratio change the location and magnitude of the peak stresses in the tow. Most of the peak stresses exist either at the edge of the tow or in the region of undulation. Any stress component can play a significant role in failure depending upon the in-plane and out-of-plane shear and normal strength allowables. The percentage of the tow that has stresses larger than those in an equivalent laminate increases with an increased waviness ratio for ±25˚ and ±45˚ braids. For the considered range of parameters, 9-45% of the tow has larger stresses than the equivalent lamina.

References

1 Naik, R. A. (1995): "Failure analysis of woven and braided fabric reinforced composites", *Journal of Composite Materials*, Vol. 29, pp. 2334-2363.

2 Blackketter, D. M., Walrath, D. E. and Hansen A. C. (1993): "Modeling damage in a plain weave fabric-reinforced composite material", *Journal of Composites Technology & Research*, Vol. 15(2), pp. 136-142.

3 Kollegal, M. G. and Sridharan, S. (2000): "Strength prediction of plain woven fabrics", *Journal of Composite Materials*, Vol. 34(3), pp. 240-257.

4 Whitcomb, J. D. and Tang, X. (2000): "Predication of progressive failure of woven composites", in *Proceedings of the ASME*, Aerospace Division, AD-Vol. 63, pp. 21-29.

5 Vandurzen, P., Ivens, J. and Verpoest, I. (1998): "Micro-stress analysis of woven fabric composites", *Journal of Composites Materials,* Vol. 32(7), pp. 623-651.

6 Kelkar, A. D. and Whitcomb, J. D. (2003): "Annual Report submitted to the Federal Aviation Administration (FAA) for the Grant No. FA03- 01- C00033".

7 Tang, X. and Whitcomb, J. D. (2003): "General techniques for exploiting periodicity and symmetries in micromechanics analysis of textile composites", *Journal of Composite Materials,* 37(13), pp. 1167-1190.

8 Goyal, D., Tang, X. and Whitcomb, J. D. (2004): "Effect of various parameters on effective engineering properties of 2x2 braided composites", accepted for publication in *Journal for Mechanics of Advanced Materials and Structures.*